Supporting Information

# Dynamic by Design: Unlocking Full Relaxation in Disulfide Epoxy Networks

*Paula Fanlo, Osman Konuray, Olaia Ochoteco, Marta Ximenis, Alaitz Rekondo, Hans Jürgen Grande, Xavier Fernández-Francos, Haritz Sardon and Alaitz Ruiz de Luzuriaga*

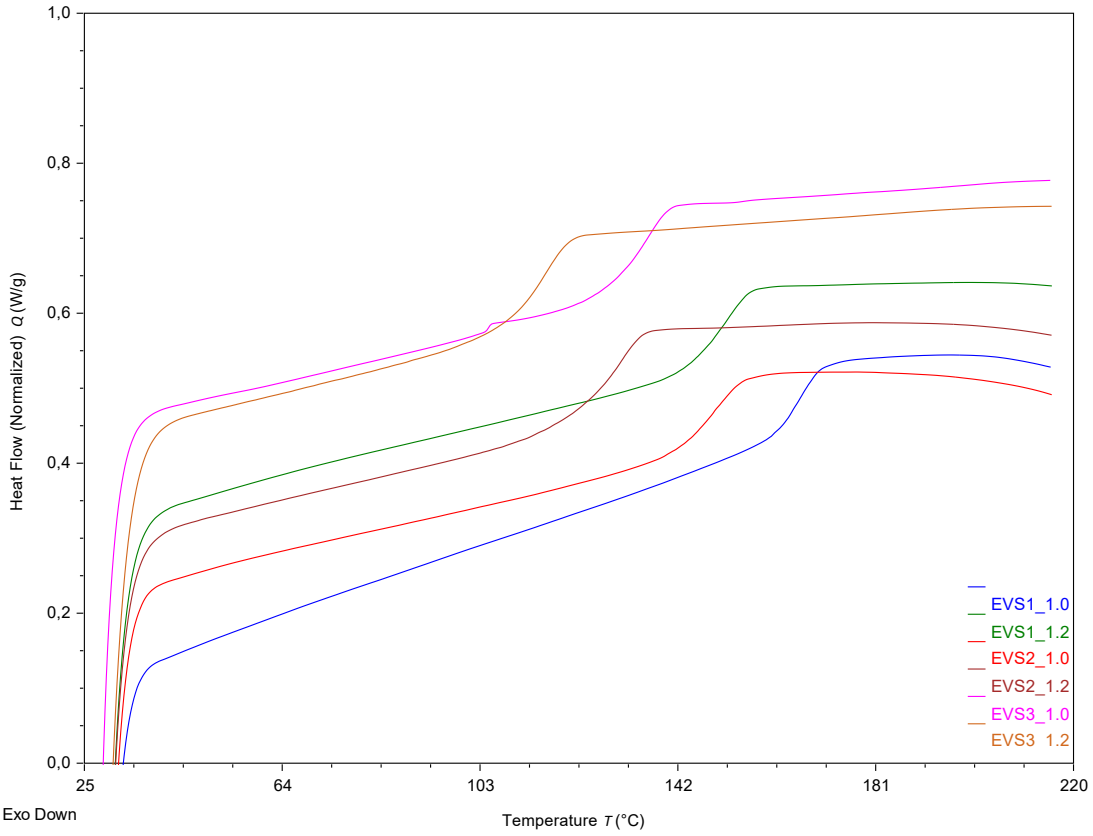


**Figure S1**. The complete cure of the epoxy vitrimers (EVS1_1.0, EVS1_1.2, EVS2_1.0, EVS2_1.2, EVS3_1.0 and EVS3_1.2) by differential scanning calorimetry (DSC).

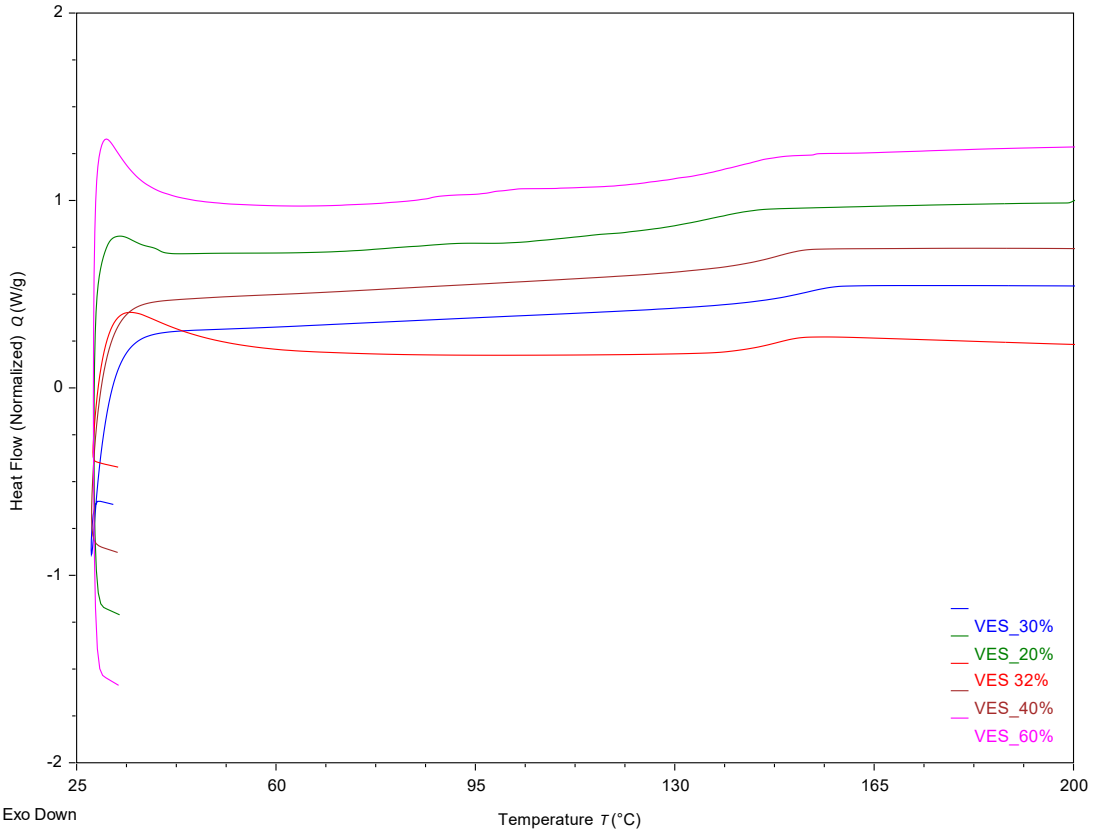


**Figure S2**. The complete cure of the epoxy vitrimers (VES_60%, VES_40%, VES_32%, VES_30% and VES_20%) by differential scanning calorimetry (DSC).

**Table S1.** Formulation of studied epoxy vitrimers.

| Sample | Stoichiometry NH2/epoxy | $T_{g\ DSC}$ (°C) | $T_{g\ DMA}$ (°C) | $T_{d,\ onset*}$ (°C) |
|---|---|---|---|---|
| EVS1 | 1.0 | 166 | 170 | 290 |
| | 1.2 | 152 | 149 | 280 |
| EVS2 | 1.0 | 149 | 150 | 268 |
| | 1.2 | 131 | 132 | 255 |
| EVS3 | 1.0 | 136 | 137 | 255 |
| | 1.2 | 115 | 123 | 253 |

**The temperature of 5 wt% loss of material.*

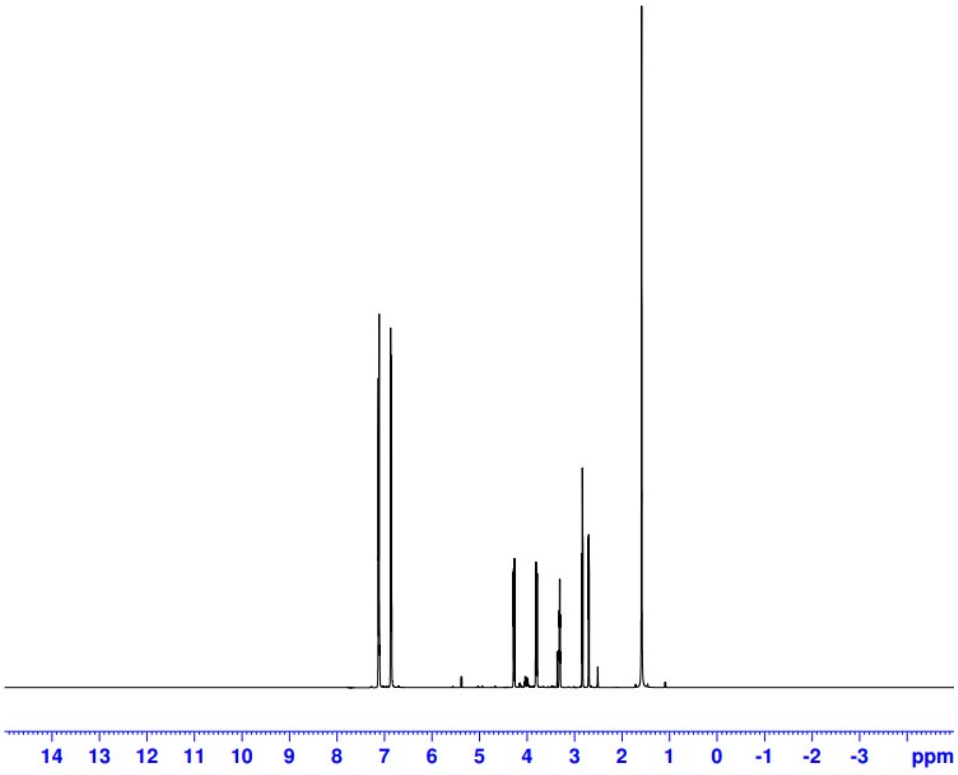


**Figure S3**. The NMR of the DGEBA used, HEXION 828.

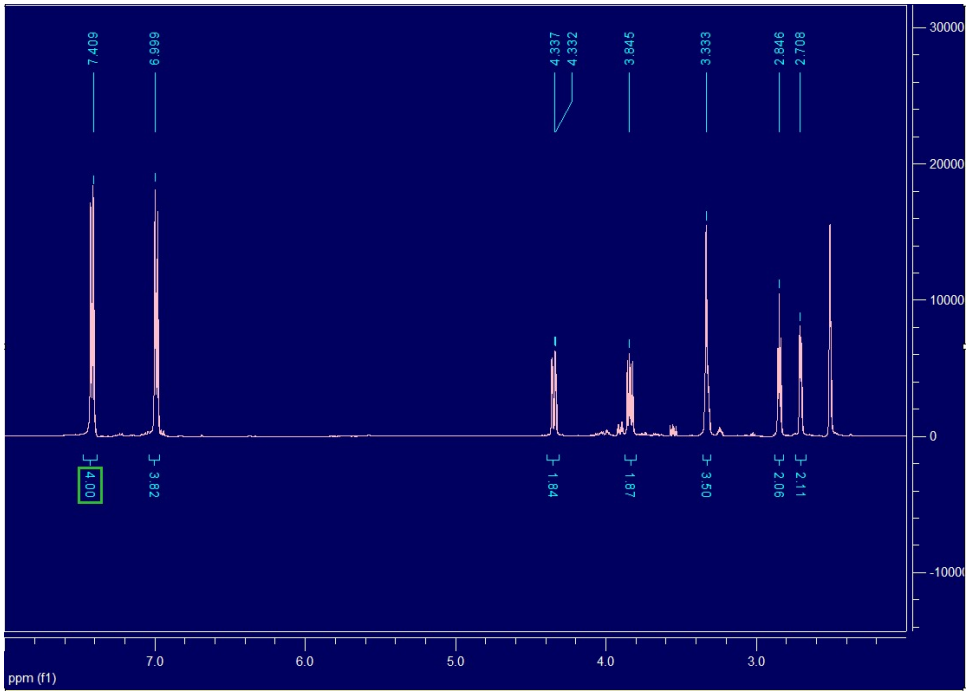


**Figure S4**. The NMR of the bis(4-glycidyloxyphenyl)disulfide.

**Structural model for the analysis of EVS1 system (DGEBA+4AFD)**

The network is modeled as composed of small structural fragments that combine according to certain rules giving way to new fragments. Since the masses of each

fragment are known, the molecular weight of the polymer can be calculated as a function of curing time. Other network parameters such as crosslinking density can also be calculated. The mathematical procedure is based on the recursive methodology devised by Miller and Macosko [1], and is similar to the one used by Williams and co-workers [2]

The structural model includes the contribution of both epoxy-amine and etherification reactions, in a similar way to the work of Riccardi and Williams [3]. In spite of the simplified model of the polyetherification network, the fragment approach produces a more accurate description of the polyetherification concomitant to epoxy-amine addition in comparison with more rigorous approaches, as shown by Williams et al. [4]

**EVS1 system (DGEBA+4AFD)**

A set of structural fragments has been defined with connecting bonds accounting for the state of reaction and the symmetry of the original components. The epoxy-amine reaction converts amine hydrogens into A+ bonds, which are connected with A- bonds that result from ring opening of the epoxy groups. The polyetherification reaction leads to the formation of E+ and E- bonds which are connected. DG* and S-> bonds represent symmetry of the fragments and are connected within themselves in a random fashion.

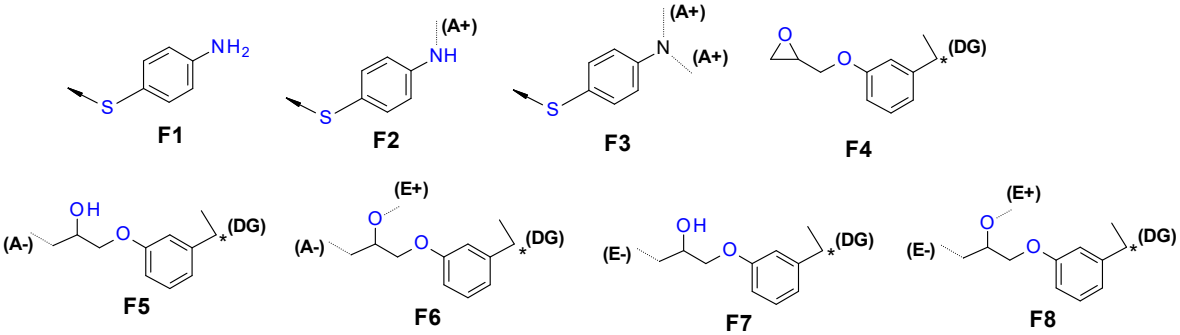


**Scheme S1.** The definition of structural fragments for the EVS1 system.

A kinetic model, inspired by the results of other researchers, [5–7] has been used to determine the evolution of structural fragments during the reactions, as illustrated in Scheme 2. The first two reactions are the epoxy-amine additions involving the primary and the secondary amines, respectively. The third and fourth reaction represent the etherification process involving different hydroxyl groups present in the system.

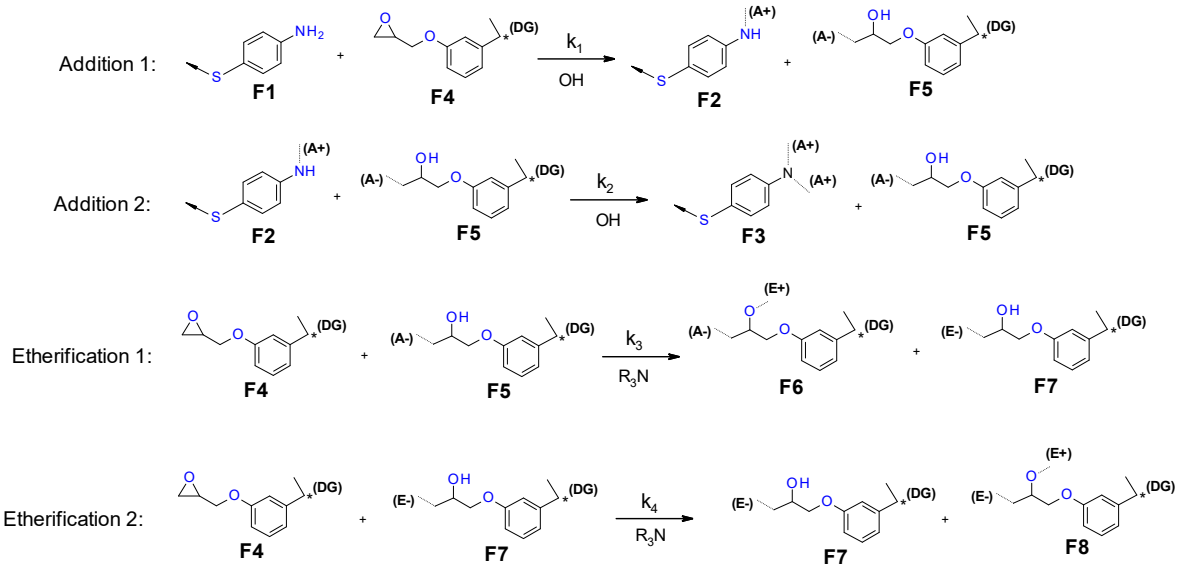


**Scheme S2.** The epoxy-amine curing reactions. The addition of a primary amine (addition 1) produces a secondary amine which reacts further to yield the tertiary amine. Both addition reactions are catalyzed by hydroxyls forming as the curing progresses. The polyethers propagate via hydroxyls on either the amine-added epoxy (Etherification 1) or the epoxy homopolymer (Etherification 2). Both etherifications are assumed to be catalyzed by the tertiary amines formed.

For the sake of simplicity, the effect of complex formation on reaction kinetics [8,9] has been neglected, and in consequence the catalytic effect of hydroxyl and tertiary amines has been modelled in a simple way. Diffusion effects are not considered either. It is also assumed that the rate constants follow Arrhenius law:

$$k_i = k_{0,i} \cdot \exp\left(-\frac{E_{A,i}}{RT}\right)$$

The set of ordinary differential equations governing the reaction kinetics are as follows:

$$\frac{d[F1]}{dt} = -\left(k_1 + k_{OH,1} \cdot [OH]\right) \cdot (2 \cdot [F1]) \cdot [F4]$$

$$\frac{d[F2]}{dt} = \left(k_1 + k_{OH,1} \cdot [OH]\right) \cdot (2 \cdot [F1]) \cdot [F4] - \left(k_2 + k_{OH,2} \cdot [OH]\right) \cdot [F2] \cdot [F4]$$

$$\frac{d[F3]}{dt} = \left(k_2 + k_{OH,2} \cdot [OH]\right) \cdot [F2] \cdot [F4]$$

$$\frac{d[F4]}{dt} = -\left(k_1 + k_{OH,1} \cdot [OH]\right) \cdot (2 \cdot [F1]) \cdot [F4] - \left(k_2 + k_{OH,2} \cdot [OH]\right) \cdot [F2] \cdot [F4] \cdot [F3] - k_4 \cdot [F7] \cdot [F4] \cdot [F3]$$

$$\frac{d[F5]}{dt} = \left(k_1 + k_{OH,1}\cdot[OH]\right)\cdot(2\cdot[F1])\cdot[F4] + \left(k_2 + k_{OH,2}\cdot[OH]\right)\cdot[F2]\cdot[F4]\cdot[F3]$$

$$\frac{d[F6]}{dt} = k_3\cdot[F5]\cdot[F4]\cdot[F3]$$

$$\frac{d[F7]}{dt} = k_3\cdot[F5]\cdot[F4]\cdot[F3]$$

$$\frac{d[F8]}{dt} = k_4\cdot[F7]\cdot[F4]\cdot[F3]$$

where $[OH] = [F5] + [F7]$.

The following relations hold true for bond concentrations (bond numbers, hereafter):

$$\left[A_+\right] = [F1] + [F2] + 2\cdot[F3]$$

$$\left[A_-\right] = [F5] + [F6] = \left[A_+\right]$$

$$\left[E_+\right] = [F6] + [F8]$$

$$\left[E_-\right] = [F7] + [F8] = \left[E_+\right]$$

$$[S] = [F1] + [F2] + [F3] = [F1]_0$$

$$[DG] = [F4] + [F5] + [F6] + [F7] + [F8] = [F4]_0$$

The initial concentration of amine and epoxy components are related using an epoxy:amine equivalent ratio as:

$$r_{epoxy} = \frac{[F4]_0}{2\cdot[F1]_0}$$

The subscript 0 indicates the beginning of the reaction. The amine ratio is determined as $r_{amine} = {}^1/_{r_{epoxy}}$.

The initial concentrations are calculated from:

$$[F4]_0 = \frac{r_{epoxy}}{0.5\cdot M_{F1} + r_{epoxy}\cdot M_{F4}} \qquad [F1]_0 = \frac{[F4]_0}{2\cdot r_{epoxy}}$$

Where $M_{F1}$ is the mass of the monoamine fragment F1, and $M_{F4}$ is the mass of the monoepoxy fragment F4. No other fragment is present initially.

The ratio of rate constants of the secondary and primary amines $k_2/k_1$ is taken as 0.5, a value similar to reported in earlier works with aromatic diamines[5]. It is assumed that

catalysis by hydroxyls is the dominating mechanism for both addition reactions. Thus, it was assumed that $k_{OH,1} = 100 \cdot k_1$ and $k_{OH,2} = 100 \cdot k_2$. Etherification rate constants are assumed several orders of magnitude larger than those of additions[7]. Activation energies reported for etherification and epoxy homopolymerization are typically twice as large as that of epoxy-amine addition [5,10] which was respected in this model as well. The kinetic parameters were further optimized by calibration based on the cure times presented in earlier reports in which this epoxy-amine system is studied. It is reported that practically complete epoxy conversions are achieved within 3 hours at $150℃$ in a stoichiometric formulation [11]. The optimized kinetic parameters are given in Table S2.

**Table S2**. Summary of pre-exponential rate constants $k_{0,i}$ and activation energies $E_{A,i}$ of epoxy-addition (subscript 1) and etherification reactions (subscripts 3), and related values of remaining kinetic constants: primary amine autocatalytic constants ( $k_{OH,1}$), reaction of secondary amines ($k_2$ and $k_{OH,2}$) and additional etherification constant ($k_3$).

| Parameter | Value (units given in parantheses) |
|---|---|
| $k_{0,1}$ | $\exp(3)(kg \cdot s/mol)$ |
| $E_{A,1}$ | $60(kJ/mol)$ |
| $k_{0,3}$ | $\exp(15)(kg^2 \cdot s/mol^2)$ |
| $E_{A,3}$ | $90(kJ/mol)$ |
| $k_{OH,1}$ | $100 \cdot k_1\ (kg^2 \cdot s/mol^2)$ |
| $k_2$ | $0.5 \cdot k_1 (kg \cdot s/mol)$ |
| $k_4$ | $k_3\ (kg^2 \cdot s/mol^2)$ |

The set of ODEs is solved using MATLAB's ode45 routine based on the Runge-Kutta (4,5) numerical procedure. The time horizon for the computation is set as $10^5$ seconds to ensure complete reactions. The temperature was set as $150℃$. An example set of outputs is given in **Figure S3**.

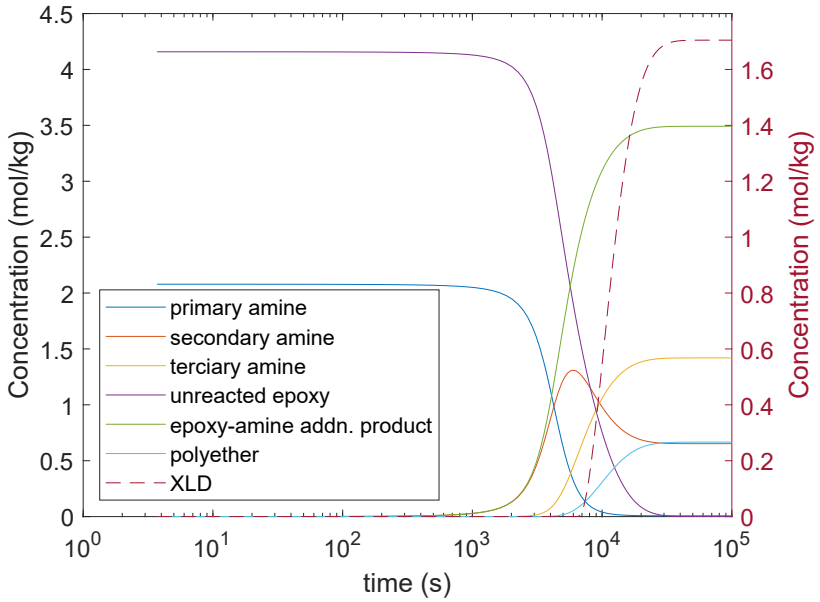


**Figure S5.** Example MATLAB output for concentrations of relevant network constituents and crosslinking density (XLD) as a function of time for the stoichiometric EVS1.

The fraction of reacted amine hydrogens with respect to the initial amine hydrogens is calculated as:

$$f_{NH} = 1 - \frac{2\cdot[F1] + [F2]}{2\cdot[F1]_0}$$

The fraction of epoxy reacted via etherification with respect to the total epoxy reacted is calculated from the number of fragments having E+ bonds (or E- bonds) as:

$$f_{ether} = \frac{[F6] + [F8]}{[F4]_0 - [F4]} = \frac{[F7] + [F8]}{[F4]_0 - [F4]}$$

The crosslinking density (XLD) is calculated using the following equation:

$$XLD = n_{EANS} = 3/2\cdot(1 - 2/3)\cdot n_{cross} = n_{cross}/2$$

$n_{EANS}$ is the concentration (or number) of elastically active network strands, the definition of which is based on the following assumptions: 1) All the crosslinks, $n_{cross}$, are tri-functional, 2) Each crosslinking point is shared by two network strands, and 3) Network strands fluctuate according to the phantom network model [12,13].

$n_{cross}$ is calculated from the extinction probabilities of the different bonds, $Z_j$, as:

$$n_{cross} = \emptyset_3[F3](1 - Z_{A+})^2(1 - Z_S) + \emptyset_6[F6](1 - Z_{A-})(1 - Z_{E+})(1 - Z_{E-})(1 - Z_{DG})$$

The $Z_j$ are the extinction probabilities that represent the likelihood that a bond of type *j* has a finite continuation. Only F3, F6 and F8 constitute crosslinks with the condition that the trifunctional branches originating from each have infinite continuations. In the expression, a set of weighing factors are used, $\emptyset_6,\emptyset_8)$ with the set of values $(1,3,3)$. These account for the distortion effect of the polyether network on the crosslinking density. For further discussion of this aspect, reader is directed to cited literature [14].

The set of $Z_j$ are calculated recursively from the following nonlinear set of equations:

$$Z_{A+} = P^{A-}_5 \cdot Z_{DG} + P^{A-}_6 \cdot Z_{E+} \cdot Z_{DG}$$

$$Z_{A-} = P^{A+}_2 \cdot Z_S + P^{A+}_3 \cdot Z_{A+} \cdot Z_S$$

$$Z_{E+} = P^{E-}_7 \cdot Z_{DG} + P^{E-}_8 \cdot Z_{E+} \cdot Z_{DG}$$

$$Z_{E-} = P^{E+}_6 \cdot Z_{A-} \cdot Z_{DG} + P^{E+}_8 \cdot Z_{E-} \cdot Z_{DG}$$

$$Z_S = P^S_1 + P^S_2 \cdot Z_{A+} + P^S_3 \cdot Z_{A+}{}^2$$

$$Z_{DG} = P^{DG}_4 + P^{DG}_5 \cdot Z_{A-} + P^{DG}_6 \cdot Z_{A-} \cdot Z_{E+} + P^{DG}_7 \cdot Z_{E-} + P^{DG}_8 \cdot Z_{E+} \cdot Z_{E-}$$

Here, the $P^j_i$ is the so-called "fishing" probability for fragment i (1 to 8), and bond type j (A+, A-, E+, E-, DG, or S) and is defined as

$$P^j_i = \frac{n^j_i}{\sum_i n^j_i}$$

where $n^j_i$ represents the number of j bonds in a fragment i. The following holds for each bond type j:

$$\sum_i P^j_i = 1$$

The set of $n^j_i$ can be given in matrix form as in Table S4:

**Table S3.** Number of bonds in each structural fragment for the EVS1 system.

| Fgm.\Bnd | A+ | A- | E+ | E- | S | DG |
|---|---|---|---|---|---|---|
| F1 | 0 | 0 | 0 | 0 | [F1] | 0 |
| F2 | [F2] | 0 | 0 | 0 | [F2] | 0 |
| F3 | 2*[F3] | 0 | 0 | 0 | [F3] | 0 |
| F4 | 0 | 0 | 0 | 0 | 0 | [F4] |
| F5 | 0 | [F5] | 0 | 0 | 0 | [F5] |
| F6 | 0 | [F6] | [F6] | 0 | 0 | [F6] |
| F7 | 0 | 0 | 0 | [F7] | 0 | [F7] |

| | | | | | | |
|---|---|---|---|---|---|---|
| F8 | 0 | 0 | [F8] | [F8] | 0 | [F8] |

Making use of the permanent network concept, the residual XLD can be calculated. This can be determined by assuming that all S-S bonds are cleaved. This is equivalent to assuming that the S bonds have finite continuations, and therefore $Z_S = 1$. The remaining extinction probabilities are recalculated from the same state of recursive equations by making $Z_S = 1$ and logically excluding the expression for $Z_S$. With the new set of extinction probabilities, the residual crosslinks can be calculated as:

$$n_{cross.res} = \emptyset_6[F6](1 - Z_{A-})(1 - Z_{E+})(1 - Z_{DG}) + \emptyset_8[F8](1 - Z_{E+})(1 - Z$$

And the residual crosslinking density can be calculated as:

$$XLD_{res} = \frac{n_{EANS}}{n_{EANS,res}} = \frac{n_{cross}/2}{n_{cross,res}/2} = \frac{n_{cross}}{n_{cross,res}}$$

The maximum epoxy:amine ratio $r_{epoxy}$ enabling complete stress relaxation is determined from the condition that $n_{cross,res} = 0$, which corresponds to the condition that all the extinction probabilities are $Z_i = 1$. For higher epoxy:amine ratio (lower amine content), a residual crosslinking density can be calculated, $n_{cross,res} > 0$ (leading to $XLD > 0$), corresponding to the existence of a non-trivial solution of the extinction probabilities $0 < Z_i < 1$.

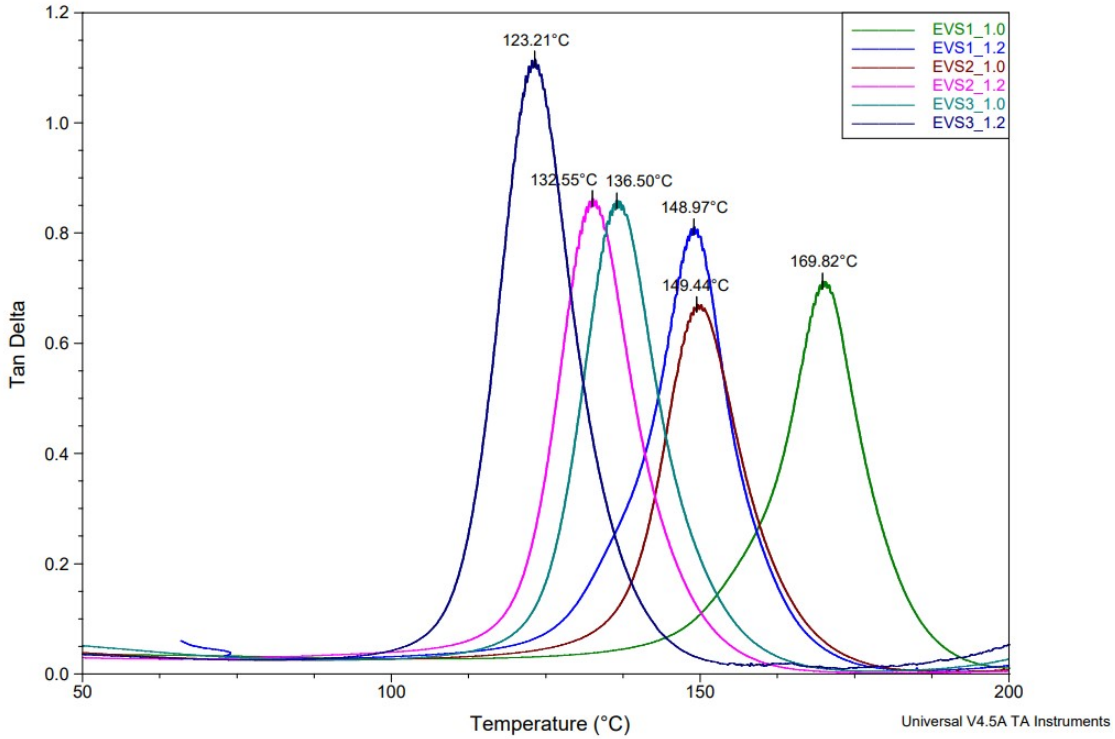


**Figure S6**. The Tan delta values from the temperature ramp of the epoxy vitrimers (EVS1_1.0, EVS1_1.2, EVS2_1.0, EVS2_1.2, EVS3_1.0 and EVS3_1.2) by dynamic mechanical analysis (DMA).

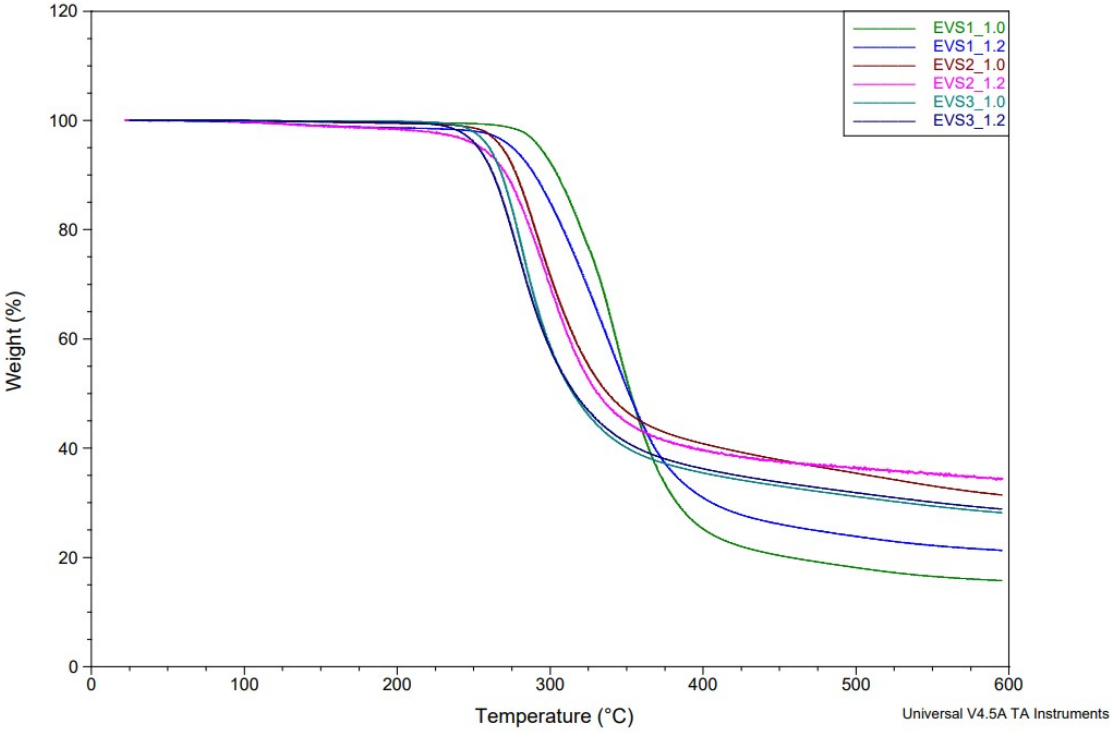


**Figure S7**. The thermogravimetric studies of the epoxy vitrimers (EVS1_1.0, EVS1_1.2, EVS2_1.0, EVS2_1.2, EVS3_1.0 and EVS3_1.2) by thermogravimetric analysis (TGA).

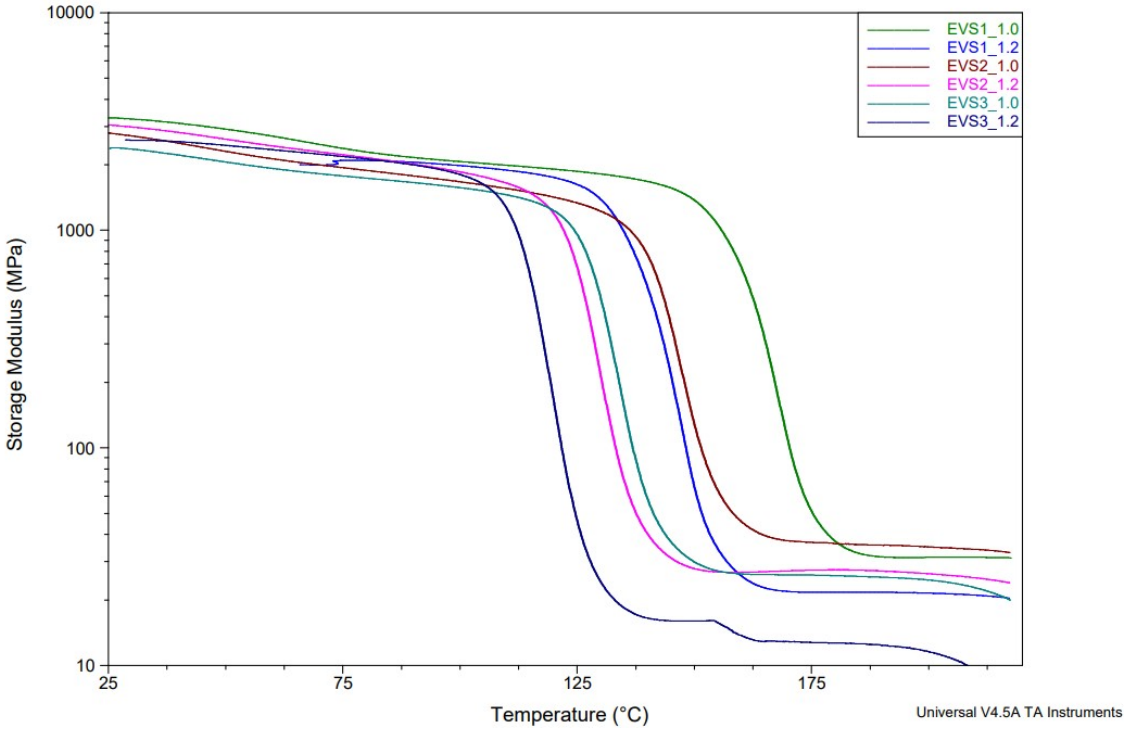


**Figure S8**. The storage modulus values from the temperature ramp of the epoxy vitrimers (EVS1_1.0, EVS1_1.2, EVS2_1.0, EVS2_1.2, EVS3_1.0 and EVS3_1.2) by dynamic mechanical analysis (DMA).

**Table S4**. Swelling tests of the the epoxy vitrimers (EVS1_1.0, EVS1_1.2, EVS2_1.0, EVS2_1.2, EVS3_1.0 and EVS3_1.2) with THF until equilibrium.

Swelling Ratio (SR): The swelling ratio quantifies the degree to which a material can absorb a solvent and is calculated as:

$$SR = (W_s - W\_d) / W\_d$$

Where:

- $W_s$ = swollen weight
- $W\_d$ = dry weight

Gel Content (GC): Gel content represents the insoluble fraction of a crosslinked polymer after extraction and is calculated as:

$$GC\ (\%) = (W\_f / W\_i) \times 100$$

Where:

- $W\_i$ = initial dry weight
- $W\_f$ = final dry weight after extraction

| Sample | Gel content % | Swelling degree % | Rubbery plateau Mpa |
|---|---|---|---|
| EVS1_1.0 | > 99 | 46 | 28 |
| EVS1_1.2 | 95 | 55 | 22 |
| EVS2_1.0 | >99 | 38 | 36 |
| EVS2_1.2 | 97 | 50 | 25 |
| EVS3_1.0 | >99 | 59 | 26 |
| EVS3_1.2 | 82 | 38 | 13 |

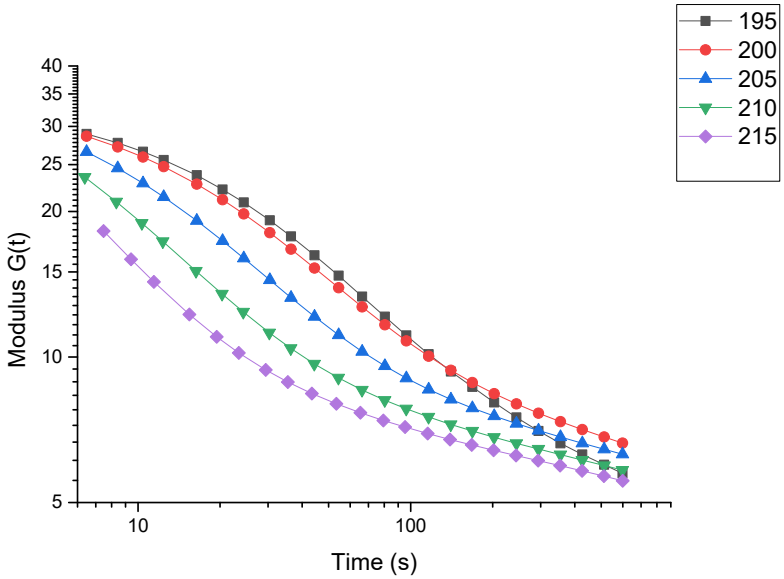


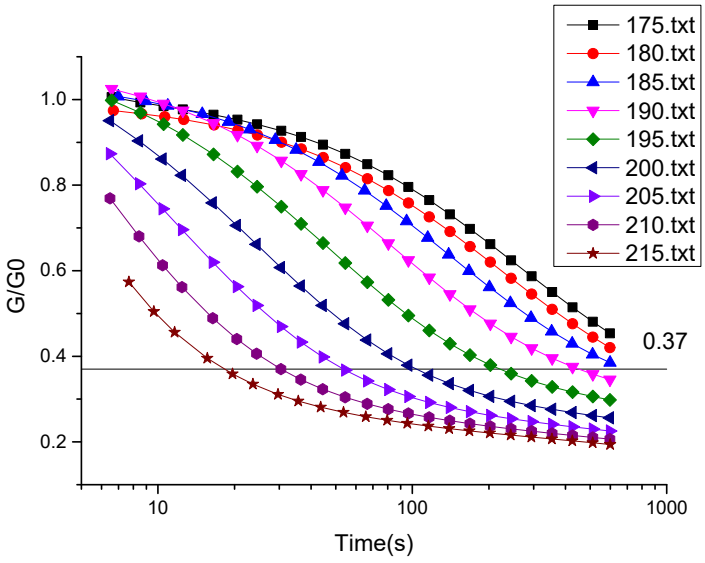

**Figure S9**. The non-normalized and the normalized TTS curves of the stress relaxation at different temperatures of the epoxy EVS1_1.0 by dynamic mechanical analysis (DMA). The normalization was done with the storage modulus' plateau obtained from the temperature ramp.

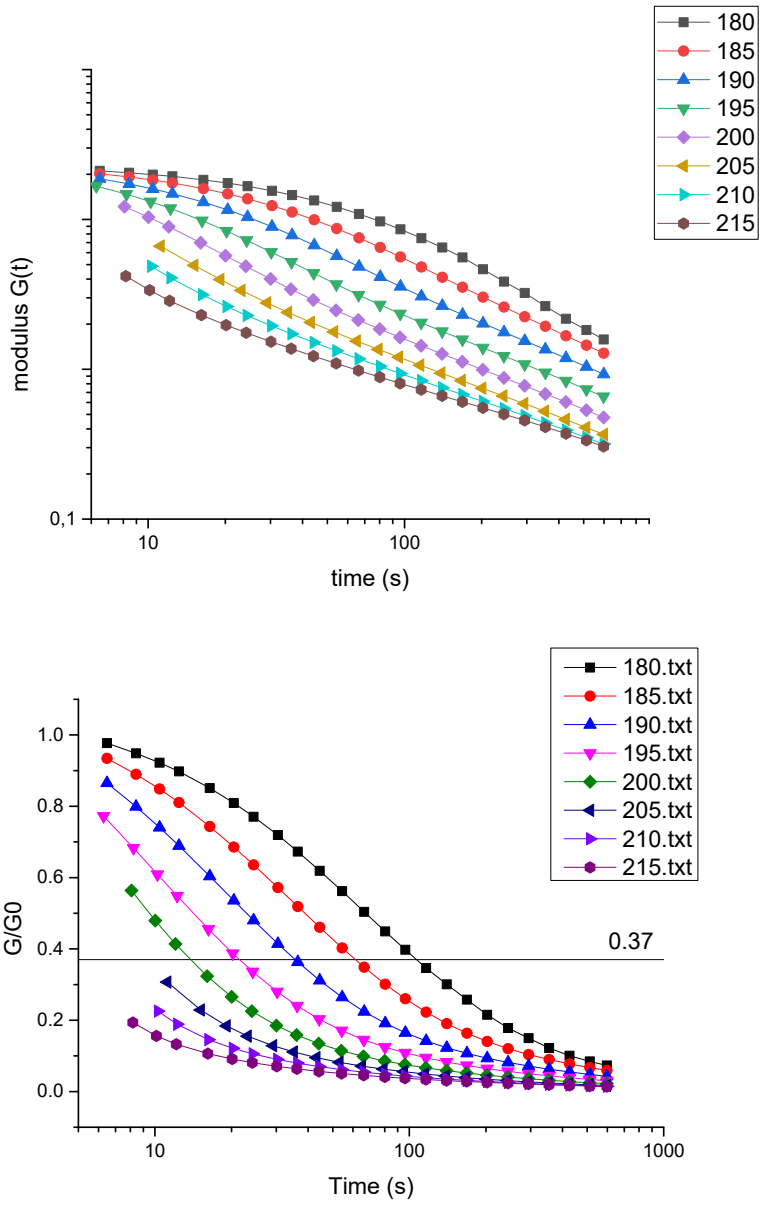


**Figure S10**. The non-normalized and the normalized TTS curves of the stress relaxation at different temperatures of the epoxy EVS1_1.2 by dynamic mechanical analysis (DMA). The normalization was done with the storage modulus' plateau obtained from the temperature ramp.

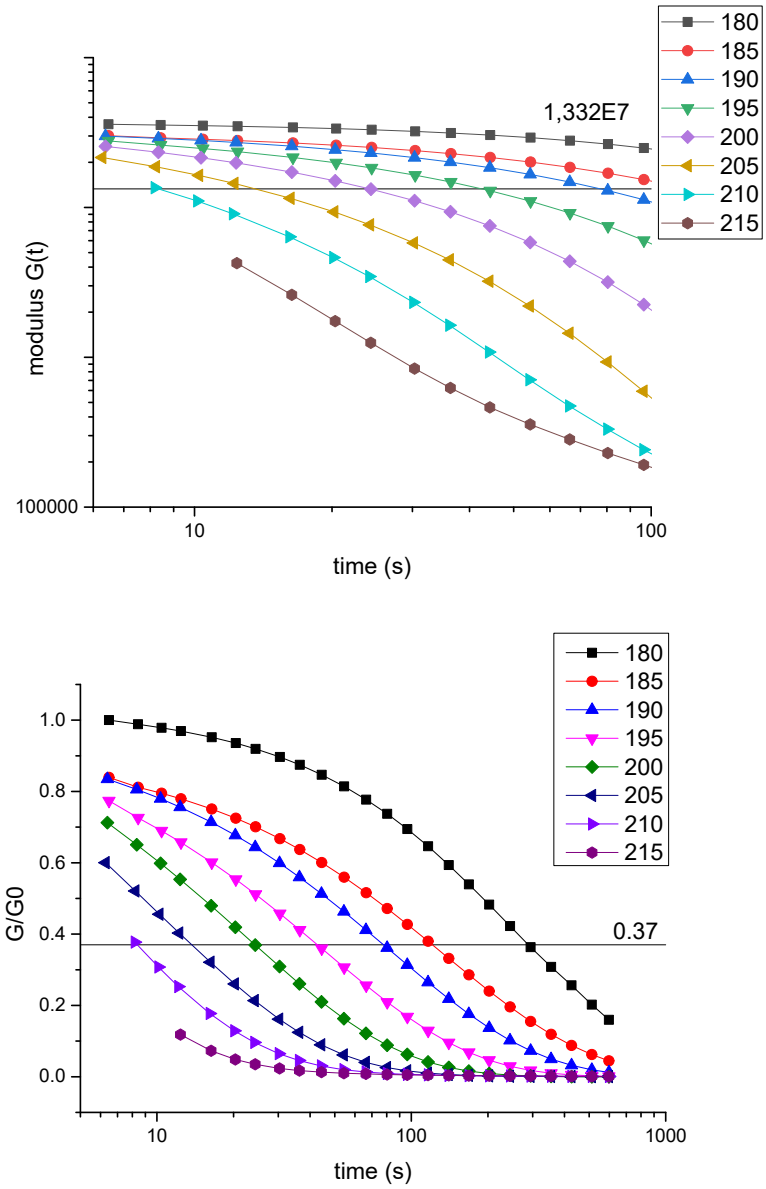


**Figure S11**. The non-normalized and the normalized TTS curves of the stress relaxation at different temperatures of the epoxy EVS2_1.0 by dynamic mechanical analysis (DMA). The normalization was done with the storage modulus' plateau obtained from the temperature ramp.

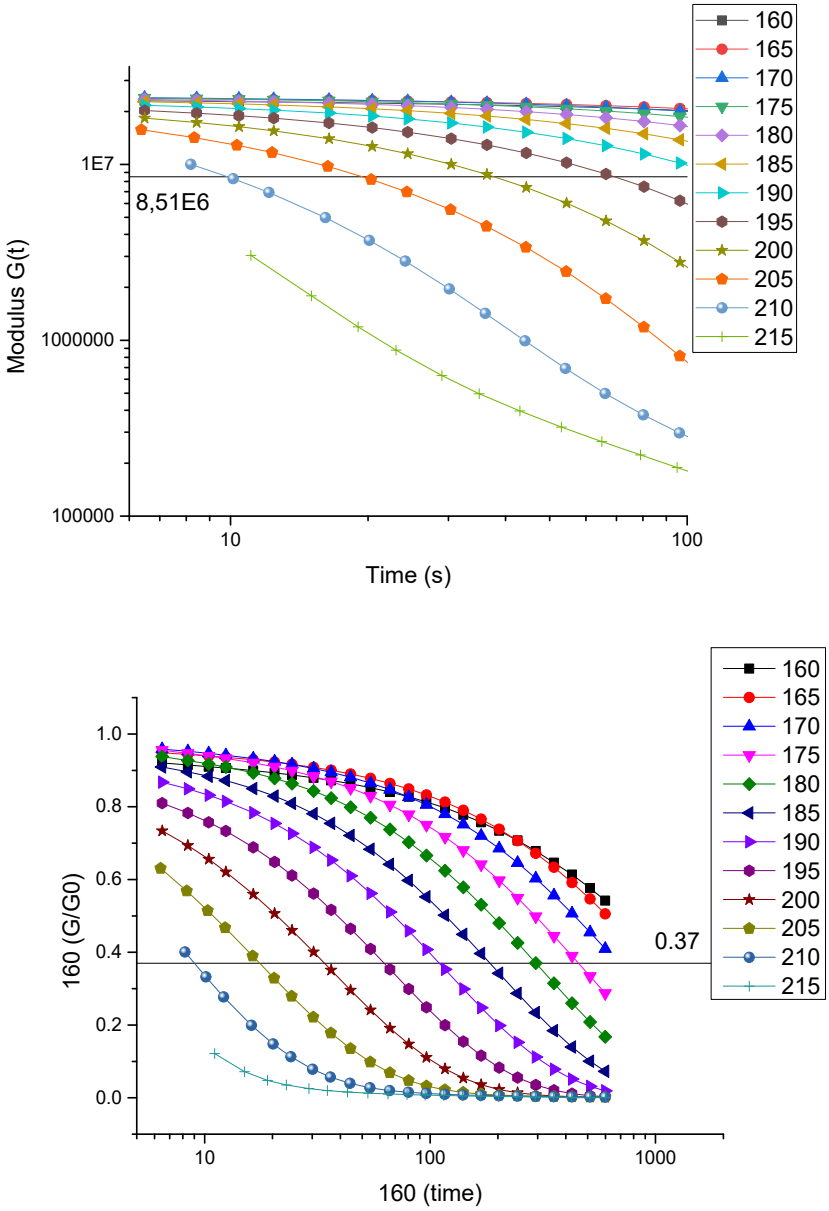


**Figure S12**. The non-normalized and the normalized TTS curves of the stress relaxation at different temperatures of the epoxy EVS2_1.2 by dynamic mechanical analysis (DMA). The normalization was done with the storage modulus' plateau obtained from the temperature ramp.

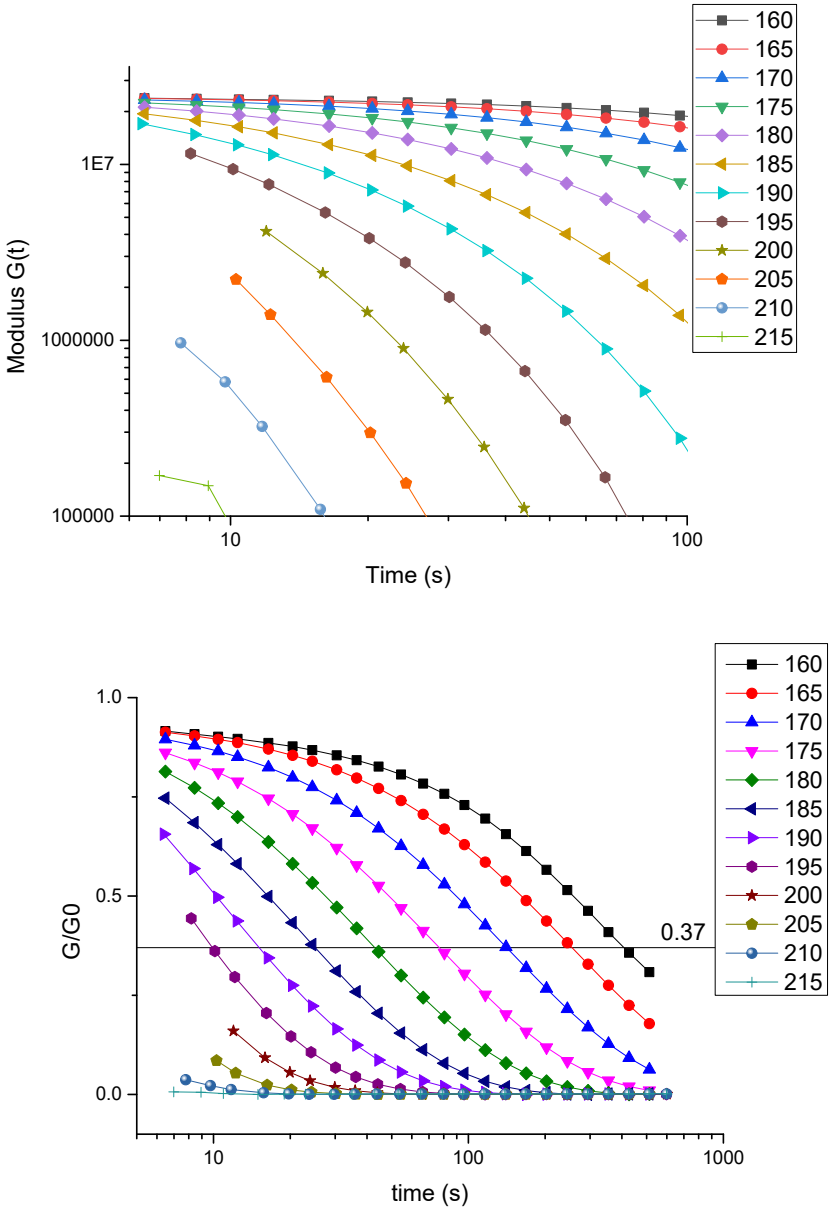


**Figure S13**. The non-normalized and the normalized TTS curves of the stress relaxation at different temperatures of the epoxy EVS3_1.0 by dynamic mechanical analysis (DMA). The normalization was done with the storage modulus' plateau obtained from the temperature ramp.

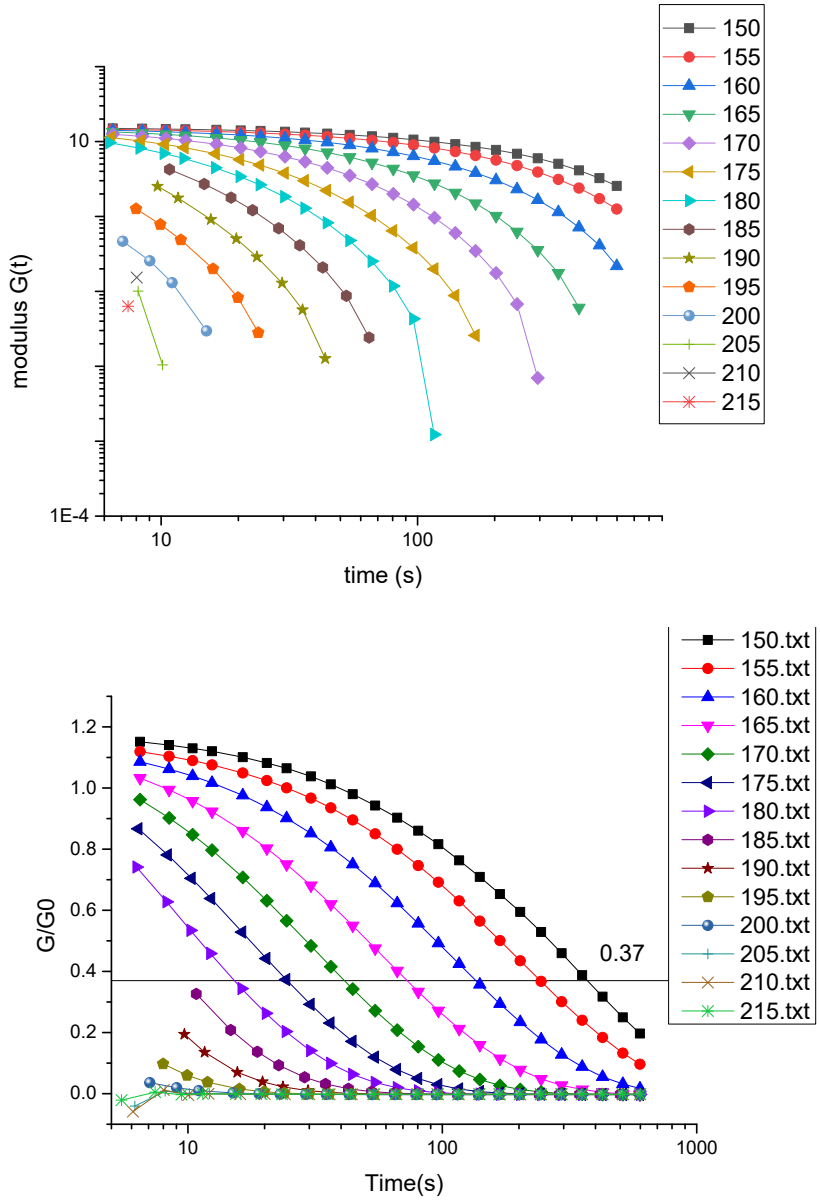


**Figure S14**. The non-normalized and the normalized TTS curves of the stress relaxation at different temperatures of the epoxy EVS3_1.2 by dynamic mechanical analysis (DMA). The normalization was done with the storage modulus' plateau obtained from the temperature ramp.

**Table S5.** The creep tests' data analyzed epoxy vitrimers (EVS1_1.0, EVS1_1.2, EVS2_1.0, EVS2_1.2, EVS3_1.0 and EVS3_1.2) by dynamic mechanical analysis (DMA).

| Sample | Stoichiometry NH2/epoxy | Above Tg | | | Below Tg |
|---|---|---|---|---|---|
| | | Initial deformation (%) | Recovery (%) | Final deformation (%) | Final deformation (%) |
| EVS1 | 1.0 | 12.6 | 1.6 | 11.0 | 0.27 |
| | 1.2 | 13.7 | 1.7 | 12.0 | 0.02 |
| EVS2 | 1.0 | 20.1 | 0.3 | 19.8 | 0.53 |
| | 1.2 | 18.1 | 1.3 | 16.8 | 0.22 |
| EVS3 | 1.0 | 26.8 | 0.2 | 26.6 | 0.28 |
| | 1.2 | 20.6 | 0.1 | 20.5 | 0.15 |

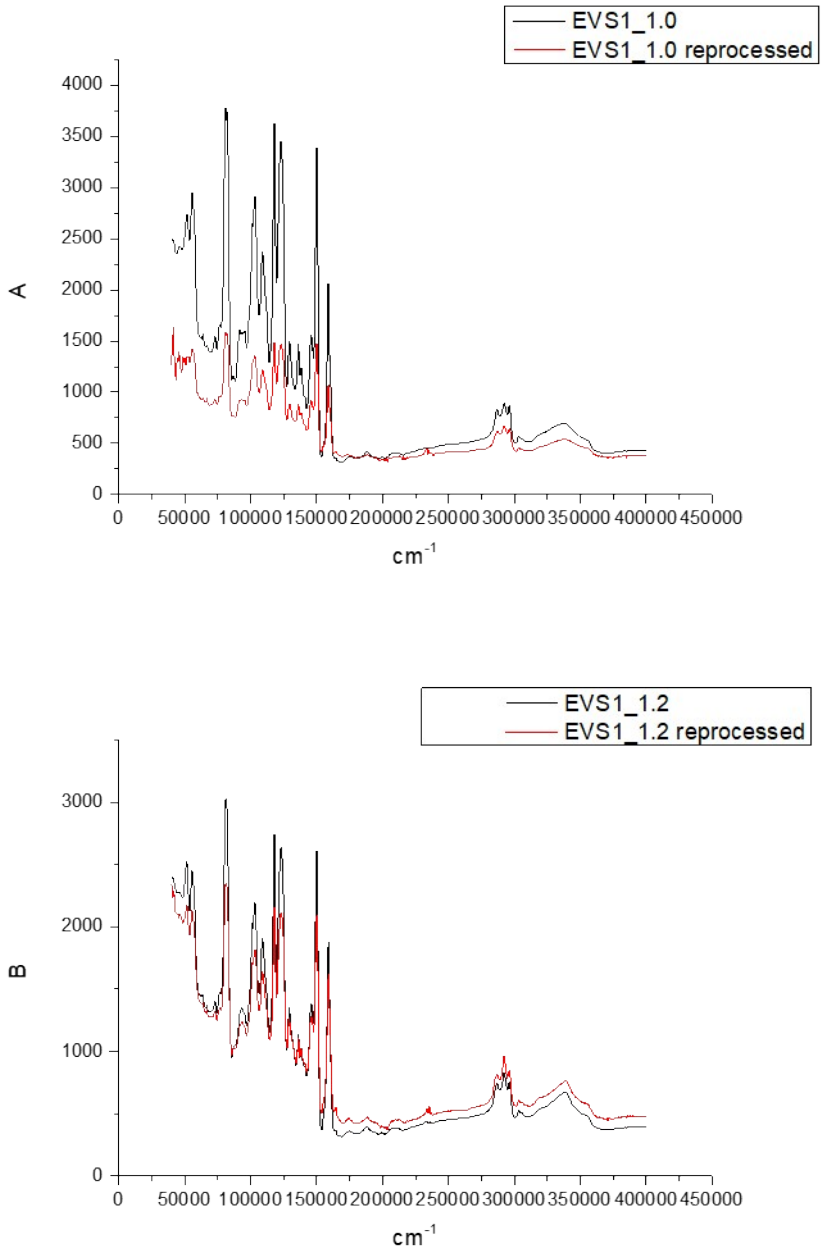


**Figure S15**. The FTIR spectrums of EVS1 vs EVS1 reprocessed.

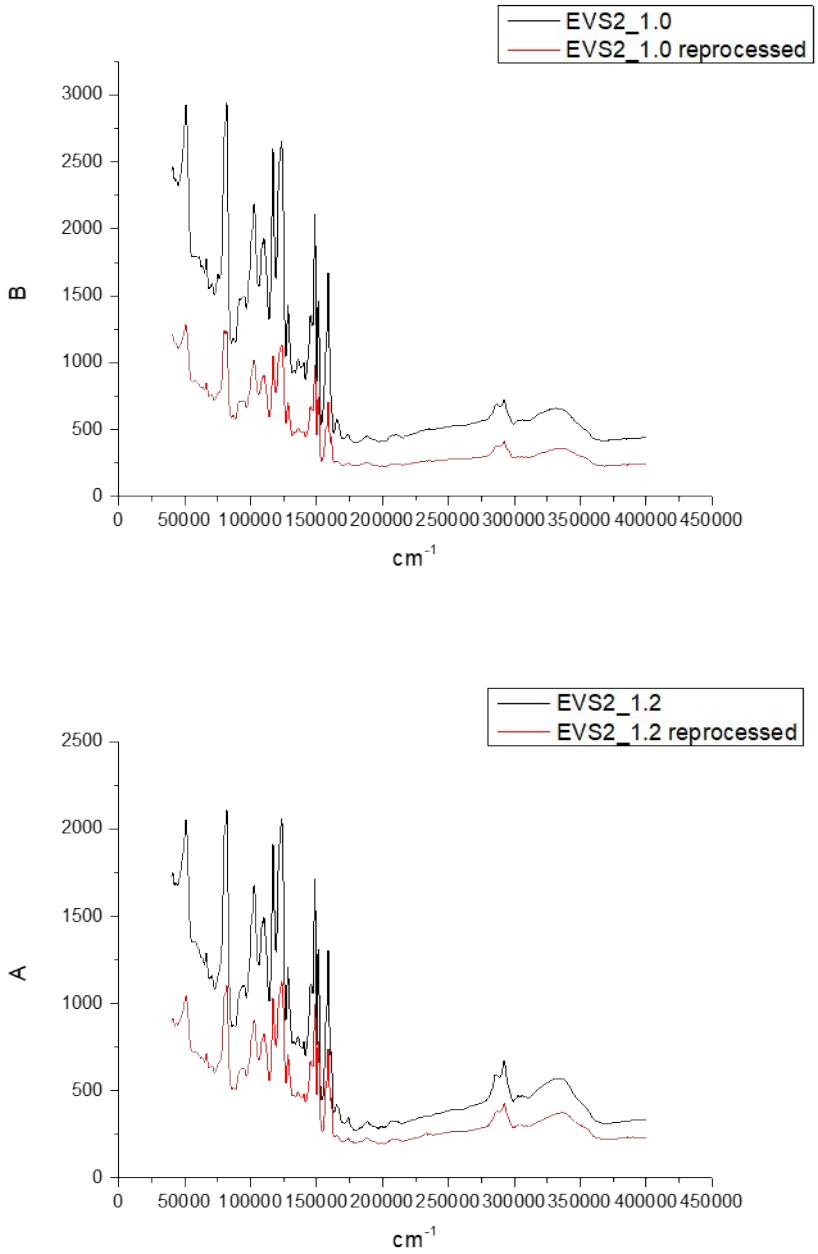


**Figure S16**. The FTIR spectrums of EVS2 vs EVS2 reprocessed.

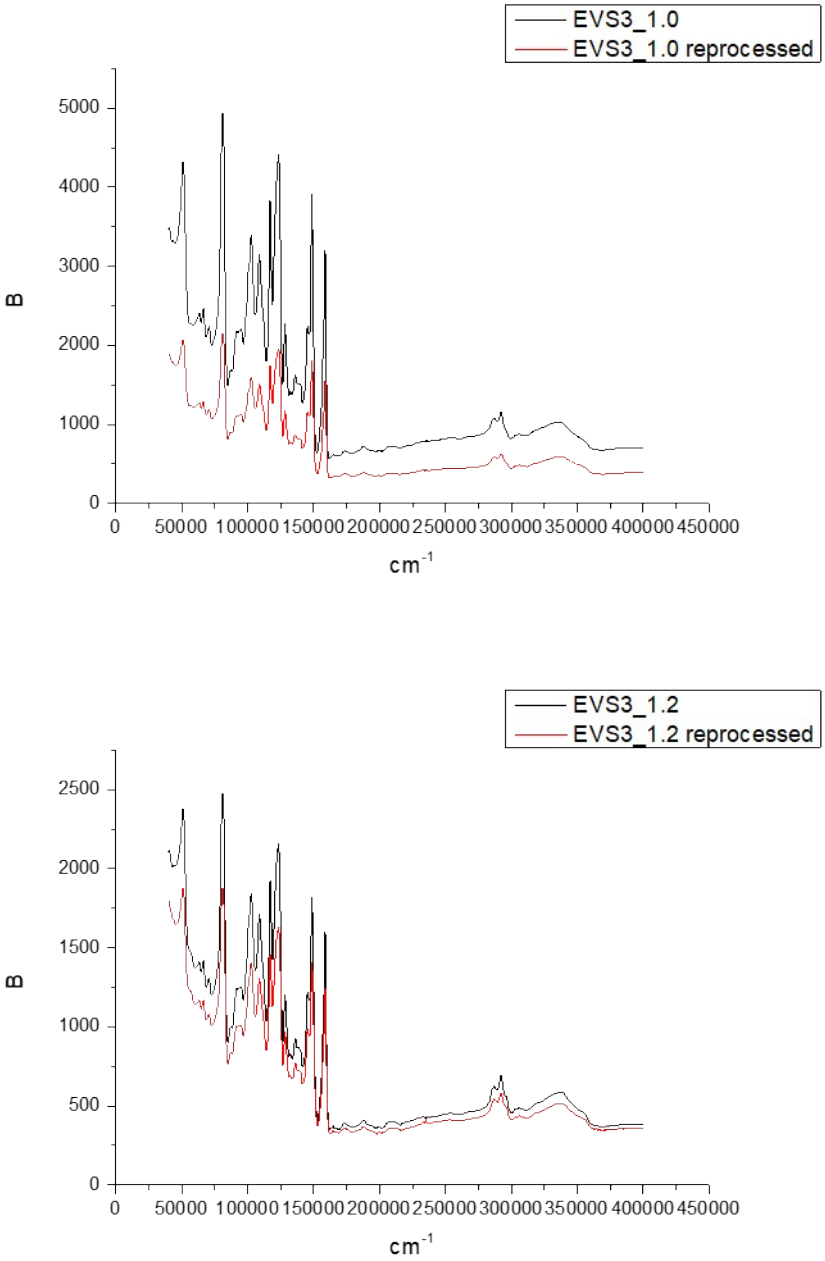


**Figure S17**. The FTIR spectrums of EVS3 vs EVS3 reprocessed.

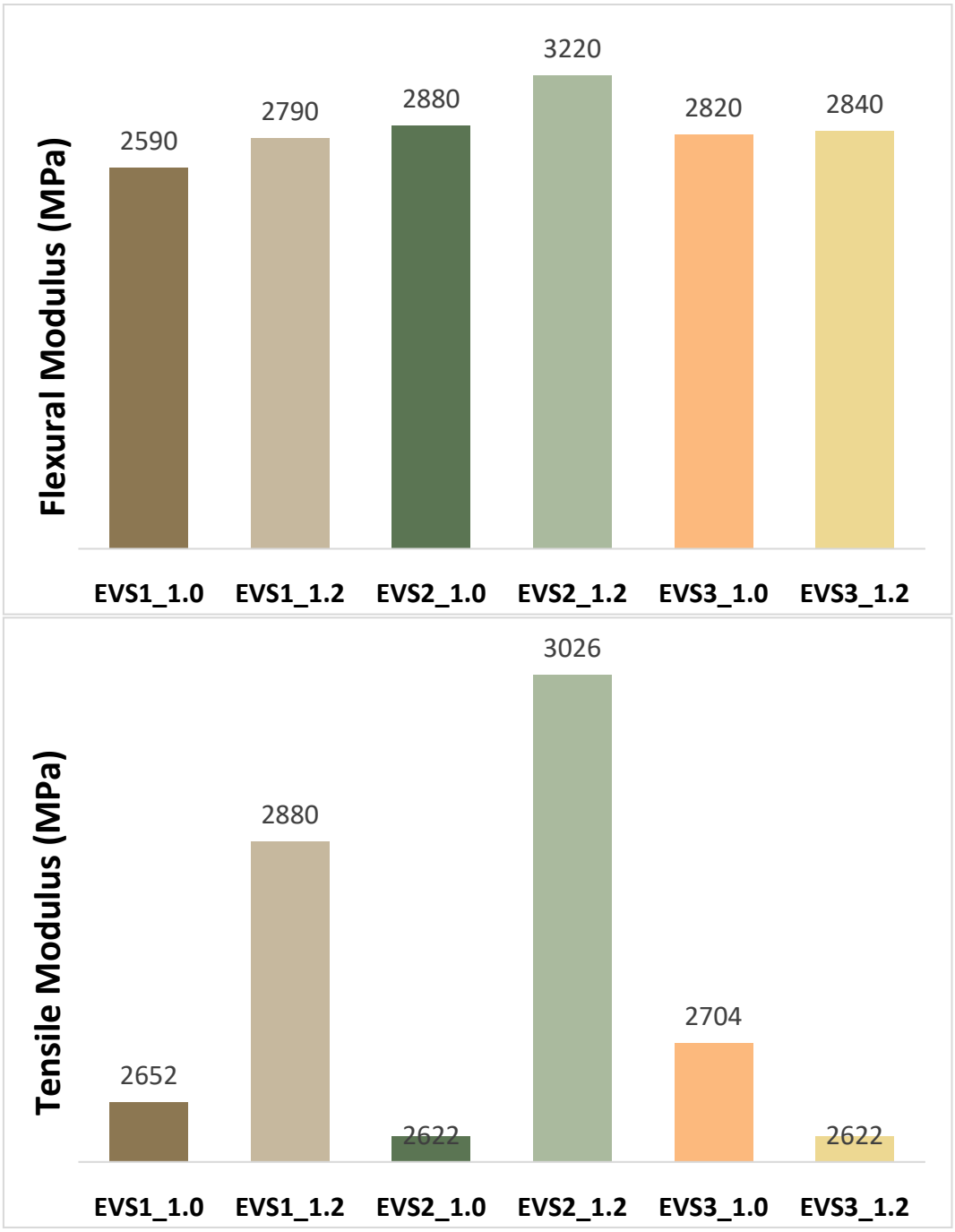


**Figure S18**. Tensile and flexural modules of all of the formulations.

**Structural model for the analysis of EVS2 system (BGPDS/DGEBA+MDA)**

The methodology for the analysis of EVS2 system is similar to that used for the EVS1 system. A new set of structural fragments are defined as in **Scheme S3**. Amine fragments F1 to F3 are identical to those defined for EVS1 with the S bond replaced by a non-dynamic C-C bond denoted as RX*. Whereas fragments F4 to F8 are identical to those defined for EVS1 system, fragments F9 to F13 represent the different reaction states of the dynamic epoxy component.

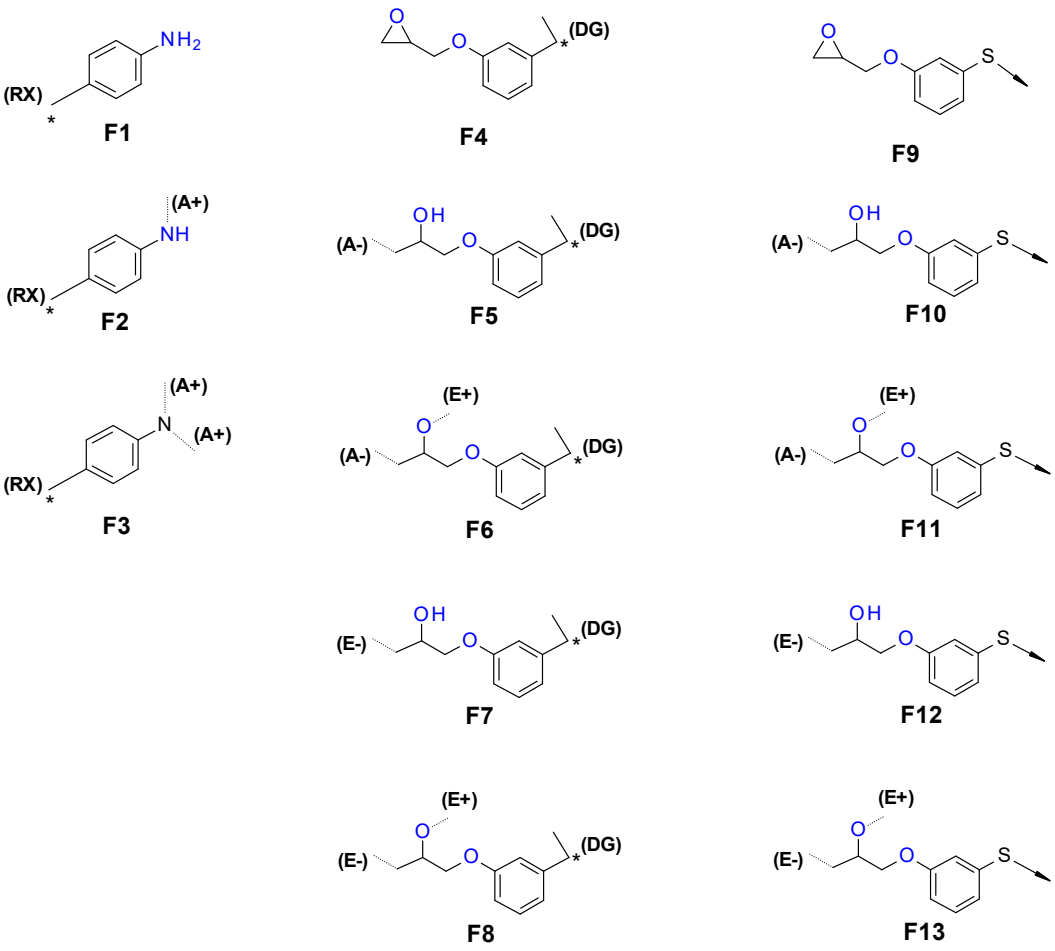


**Scheme S3.** Structural fragments for the EVS2 system.

The following relations hold:

$$[A_+] = [F1] + [F2] + 2\cdot[F3]$$

$$[A_-] = [F5] + [F6] + [F10] + [F11] = [A_+]$$

$$[E_+] = [F6] + [F8] + [F11] + [F13]$$

$$[E_-] = [F7] + [F8] + [F12] + [F13] = [E_+]$$

$$[RX] = [F1] + [F2] + [F3] = [F1]_0$$

$$[DG] = [F4] + [F5] + [F6] + [F7] + [F8] = [F4]_0$$

$$[S] = [F9] + [F10] + [F11] + [F12] + [F13] = [F9]_0$$

The initial concentration of amine and epoxy components are related using an epoxy:amine equivalent ratio as:

$$r_{epoxy} = \frac{[F4]_0 + [F9]_0}{2\cdot[F1]_0}$$

A fraction of dynamic component is defined as:

$$f_d = \frac{[F9]_0}{[F4]_0 + [F9]_0}$$

The initial concentrations are calculated from:

$$[F4]_0 = \frac{r_{epoxy} \cdot (1 - f_d)}{0.5 \cdot M_{F1} + r_{epoxy} \cdot \left[(1 - f_d) \cdot M_{F4} + f_d \cdot M_{F9}\right]}$$

$$[F9]_0 = [F4]_0 \cdot f_d / (1 - f_d)$$

$$[F1]_0 = \frac{[F4]_0 + [F9]_0}{2 \cdot r_{epoxy}}$$

Where $M_{F9}$ is the mass of the dynamic epoxy fragment F9. The initial concentration of all the remaining fragments is initialized to 0.

The kinetics of formation and consumption of dynamic epoxy fragments F9 to F13 are similar to those of their non-dynamic counterparts F4 to F8. In order to simplify the kinetic model, will make use of the same set of ODEs as in the case of the EVS1 system (vide supra) by considering a global concentration of epoxy fragments $[F4*]$ to $[F8*]$ Once solved, the individual fragments can be determined as:

$$[F4] = [F4*] \cdot (1 - f_d) \qquad [F9] = [F4*] \cdot f_d$$

$$[F5] = [F5*] \cdot (1 - f_d) \qquad [F10] = [F5*] \cdot f_d$$

$$[F6] = [F6*] \cdot (1 - f_d) \qquad [F11] = [F6*] \cdot f_d$$

$$[F7] = [F7*] \cdot (1 - f_d) \qquad [F12] = [F7*] \cdot f_d$$

$$[F8] = [F8*] \cdot (1 - f_d) \qquad [F13] = [F8*] \cdot f_d$$

The initial concentration of monoepoxy species for the solution of the set of ODEs is given by $[F4*]_0 = [F4]_0 + [F9]_0$.

The capture probabilities of the different fragments are defined in the same way as before. The new matrix of values of $n_i^j$ is given as **Table S3**.

**Table S4.** Number of bonds in each structural fragment in system EVS2.

| Fgm.\Bnd | A+ | A- | E+ | E- | RX | S | DG |
|---|---|---|---|---|---|---|---|
| F1 | 0 | 0 | 0 | 0 | [F1] | 0 | 0 |
| F2 | [F2] | 0 | 0 | 0 | [F2] | 0 | 0 |
| F3 | 2*[F3] | 0 | 0 | 0 | [F3] | 0 | 0 |
| F4 | 0 | 0 | 0 | 0 | 0 | 0 | [F4] |
| F5 | 0 | [F5] | 0 | 0 | 0 | 0 | [F5] |

| | | | | | | | |
|---|---|---|---|---|---|---|---|
| F6 | 0 | [F6] | [F6] | 0 | 0 | 0 | [F6] |
| F7 | 0 | 0 | 0 | [F7] | 0 | 0 | [F7] |
| F8 | 0 | 0 | [F8] | [F8] | 0 | 0 | [F8] |
| F9 | 0 | 0 | 0 | 0 | 0 | [F9] | 0 |
| F10 | 0 | [F10] | 0 | 0 | 0 | [F10] | 0 |
| F11 | 0 | [F11] | [F11] | 0 | 0 | [F11] | 0 |
| F12 | 0 | 0 | 0 | [F12] | 0 | [F12] | 0 |
| F13 | 0 | 0 | [F13] | [F13] | 0 | [F13] | 0 |

The new set of extinction probabilities $Z_j$ is defined as:

$$Z_{A+} = P^{A-}_{5} \cdot Z_{DG} + P^{A-}_{6} \cdot Z_{E+} \cdot Z_{DG} + P^{A-}_{10} \cdot Z_s + P^{A-}_{11} \cdot Z_{E+} \cdot Z_S$$

$$Z_{A-} = P^{A+}_{2} \cdot Z_{RX} + P^{A+}_{3} \cdot Z_{A+} \cdot Z_{RX}$$

$$Z_{E+} = P^{E-}_{7} \cdot Z_{DG} + P^{E-}_{8} \cdot Z_{E+} \cdot Z_{DG} + P^{E-}_{12} \cdot Z_S + P^{E-}_{13} \cdot Z_{E+} \cdot Z_S$$

$$Z_{E-} = P^{E+}_{6} \cdot Z_{A-} \cdot Z_{DG} + P^{E+}_{8} \cdot Z_{E-} \cdot Z_{DG} + P^{E+}_{11} \cdot Z_{A-} \cdot Z_S + P^{E+}_{13} \cdot Z_{E-} \cdot Z_S$$

$$Z_{RX} = P^{RX}_{1} + P^{RX}_{2} \cdot Z_{A+} + P^{RX}_{3} \cdot (Z_{A+})^2$$

$$Z_S = P^{S}_{9} + P^{S}_{10} \cdot Z_{A-} + P^{S}_{11} \cdot Z_{A-} \cdot Z_{E+} + P^{S}_{12} \cdot Z_{E-} + P^{S}_{13} \cdot Z_{E+} \cdot Z_{E-}$$

$$Z_{DG} = P^{DG}_{4} + P^{DG}_{5} \cdot Z_{A-} + P^{DG}_{6} \cdot Z_{A-} \cdot Z_{E+} + P^{DG}_{7} \cdot Z_{E-} + P^{DG}_{8} \cdot Z_{E+} \cdot Z_{E-}$$

The new $n_{cross}$ for crosslinking density calculation:

$$n_{cross} = \emptyset_3[F3](1 - Z_{A+})^2(1 - Z_{RX}) + \emptyset_6[F6](1 - Z_{A-})(1 - Z_{E+})(1 - Z$$
$$(1 - Z_{E+})(1 - Z_{E-})(1 - Z_{DG}) + \emptyset_{11}[F11](1 - Z_{A-})(1 - Z_{E+})(1 -$$
$$+ \emptyset_{13}[F13](1 - Z_{E+})(1 - Z_{E-})(1 - Z_S)$$

with the weighing factors $(\emptyset_3, \emptyset_6, \emptyset_8, \emptyset_{11}, \emptyset_{13}) = (1,3,3,3,3)$.

The residual XLD is determined similarly by assuming that all S-S bonds are cleaved, as in the previous system, by setting $Z_S = 1$ and re-calculation of extinction probabilities excluding $Z_S$. The residual crosslinking density would be calculated as

$$n_{cross,res} = \emptyset_3[F3](1 - Z_{A+})^2(1 - Z_{RX}) + \emptyset_6[F6](1 - Z_{A-})(1 - Z_{E+})(1 - Z$$
$$(1 - Z_{E+})(1 - Z_{E-})(1 - Z_{DG})$$

The lower boundary for the fraction of BGPDS in the formulation $f_d$ enabling complete stress relaxation, is determined from the condition that $n_{cross,res} = 0$, which corresponds to the condition that $Z_i = 1$. That is, all extinction probabilities must be unity. For lower BGPDS content, a residual crosslinking density $n_{cross,res} > 0$ (leading to

$XLD > 0$) can be calculated corresponding to the existence of a non-trivial solution of the extinction probabilities such that $0 < Z_i < 1$.

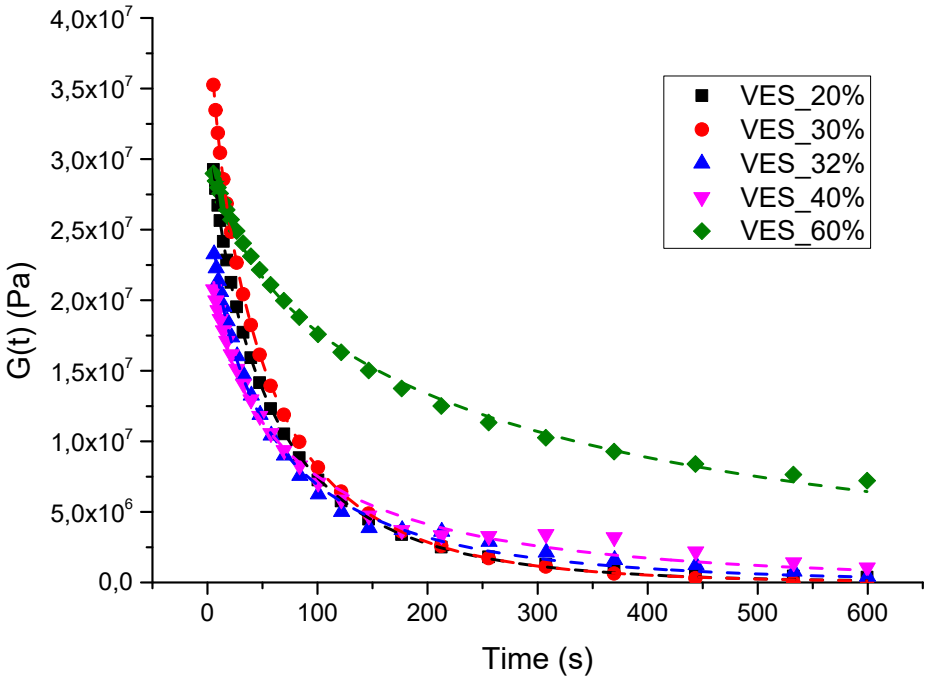


| | A | β | T | Statistics | Statistics |
|---|---|---|---|---|---|
| | Value | Value | Value | Reduced Chi-Sqr | Adj. R-Square |
| VES_20% | 3,60E+07 | 0,70623 | 52,39146 | 1,98E+10 | 0,99981 |
| VES_30% | 4,40E+07 | 0,69914 | 47,35562 | 3,85E+09 | 0,99997 |
| VES_32% | 3,15E+07 | 0,59503 | 49,62769 | 1,90E+11 | 0,99687 |
| VES_40% | 2,81E+07 | 0,54052 | 59,8304 | 3,03E+11 | 0,99321 |
| VES_60% | 3,39E+07 | 0,5259 | 228,53395 | 1,19E+11 | 0,99781 |

**Figure S19.** Stress relaxations of the VES samples fitted to KWW model. Experimental data (colored symbols) fit by a KWW model (dashed colored lines).

**REFERENCES**


1 D. R. Miller and C. W. Macosko, *Macromolecules*, 1976, **9**, 206–211.

2 J.-P. Pascault, H. Sautereau, J. Verdu and R. J. J. Williams, *Thermosetting Polymers*, Marcel Dekker, Inc., New York, 2002.

3 C. C. Riccardi and R. J. J. Williams, *Polymer (Guildf)*, 1986, **27**, 913–920.

4 R. J. J. Williams, C. C. Riccardi and K. Dušek, *Polymer Bulletin*, 1991, **25**, 231–237.

5 E. Girard-Reydet, C. C. Riccardi, H. Sautereau and J. P. Pascault, *Macromolecules*, 1995, **28**, 7599–7607.

6 C. C. Riccardi and R. J. J. Williams, *J Appl Polym Sci*, 1986, **32**, 3445–3456.

7 K. C. Cole, J. J. Hechler and D. Noel, *Macromolecules*, 1991, **24**, 3098–3110.

8 S. Swier, G. Van Assche, W. Vuchelen and B. Van Mele, *Macromolecules*, 2005, **38**, 2281–2288.

9 S. Swier, G. Van Assche and B. Van Mele, *J Appl Polym Sci*, 2004, **91**, 2814–2833.

10 J. Mijovic and J. Wijaya, *Polymer (Guildf)*, 1994, **35**, 2683–2686.

11 D. Sanchez-Rodriguez, S. Zaidi, Y. Jahani, A. Ruiz de Luzuriaga, A. Rekondo, P. Maimi, J. Farjas and J. Costa, *Polym Degrad Stab*, 2023, **217**, 110543.

12 A. J. Lesser and E. Crawford, *J Appl Polym Sci*, 1997, **66**, 387–395.

13 J. M. Charlesworth, *Polym Eng Sci*, 1988, **28**, 189–236.

14 X. Fernández-Francos, D. Santiago, F. Ferrando, X. Ramis, J. M. Salla, À. Serra and M. Sangermano, *J Polym Sci B Polym Phys*, 2012, **50**, 1489–1503.